MycoKeys 27: 21–38 (2017)
doi: 10.3897/mycokeys.27.21254
http://mycokeys.pensoft.net

RESEARCH ARTICLE

A peer-reviewed open-access journal
MycoKeys
Launched to accelerate biodiversity research

Monocillium gamsii sp. nov. and *Monocillium bulbillosum*: two nematode-associated fungi parasitising the eggs of *Heterodera filipjevi*

Samad Ashrafi[1,2], Marc Stadler[3], Abdelfattah A. Dababat[4], Katja R. Richert-Pöggeler[1], Maria R. Finckh[2], Wolfgang Maier[1]

1 *Institute for Epidemiology and Pathogen Diagnostics, Julius Kühn-Institut (JKI)–Federal Research Centre for Cultivated Plants, Braunschweig, Germany* **2** *Department of Ecological Plant Protection, Faculty of Organic Agricultural Sciences, University of Kassel, Witzenhausen, Germany* **3** *Department Microbial Drugs, Helmholtz Centre for Infection Research GmbH (HZI), Braunschweig, Germany* **4** *CIMMYT (International Maize and Wheat Improvement Centre), P.K.39 06511 Emek, Ankara, Turkey*

Corresponding author: *Samad Ashrafi* (samad.ashrafi@julius-kuehn.de; ashrafi.samad@gmail.com)

Academic editor: *C. Gueidan* | Received 27 September 2017 | Accepted 25 October 2017 | Published 1 November 2017

Citation: Ashrafi S, Stadler M, Dababat AA, Richert-Pöggeler KR, Finckh MR, Maier W (2017) *Monocillium gamsii* sp. nov. and *Monocillium bulbillosum*: two nematode-associated fungi parasitising the eggs of *Heterodera filipjevi*. MycoKeys 27: 21–38. https://doi.org/10.3897/mycokeys.27.21254

Abstract

Monocillium gamsii **sp. nov.** (Ascomycota, Hypocreales, Niessliaceae) isolated from eggs of the cereal cyst nematode *Heterodera filipjevi* is described and illustrated based on morphological and molecular phylogenetic evidence. The new taxon discovered in wheat fields in Turkey destructively parasitises nematode eggs. The infected eggs were readily colonised by the fungus, which produced microsclerotia. The fungus could be grown on artificial media and the parasitism of *M. gamsii* towards *H. filipjevi* was reproducible in vitro. Hyphae penetrating the nematode eggs entirely colonised the embryo, developed into multicellular chlamydospore and dictyochlamydospore-like structures eventually forming microsclerotia. Molecular and morphological differences and similarities between *M. gamsii* and its phylogenetically related species are discussed. *Monocillium bulbillosum* was found to be closely related to the new species. The pathogenicity of *M. bulbillosum* against *H. filipjevi* was also assayed in vitro because of its sister group relationship to *M. gamsii* revealing that this species was also capable of colonising eggs of *H. filipjevi*.

Keywords

Egg-parasitic fungi, Niessliaceae, new species, plant parasitic nematodes, taxonomy, molecular phylogeny, ITS, LSU, *rpb1*, *tef*

Introduction

Various fungi have been reported as natural enemies of plant parasitic nematodes (PPN) (Nordbring-Hertz et al. 2011; Siddiqui and Mahmood 1996; Stirling 2014). A group of these fungi infect females and egg contents of endoparasitic nematodes such as cyst nematodes (Kerry 1988; Rodríguez-Kábana and Morgan-Jones 1988), which are biotrophic plant pathogens establishing a long-term parasitic interaction with their host plants. The unique sedentary life style of this group of PPN render them especially vulnerable of being colonised by their natural enemies (Lopez-Llorca et al. 2008). Cyst nematodes are globally distributed and were the first group of PPN reported to be parasitised by fungi (Kühn 1877), which spurred investigations to find additional nematode-antagonistic fungi ever since [(Tribe 1977) and references therein]. Most egg-parasitic fungi belong to the ascomyceteous Hypocreales, e.g. *Pochonia chlamydosporia* (Goddard) Zare & W. Gams, *Metapochonia rubescens* (Zare, W. Gams & López-Llorca) Kepler, S.A. Rehner & Humber, *Lecanicillium lecanii* (Zimm.) Zare & W. Gams, *Metarhizium* spp., *Purpureocillium lilacinum* (Thom) Luangsa-ard, Houbraken, Hywel-Jones & Samson, and *Trichoderma* spp. (Kerry and Hirsch 2011; Khan et al. 2006; Szabó et al. 2012; Zhang et al. 2014). In contrast, none of the second important group of nematode-antagonistic Ascomycota, the Orbiliomycetes (Baral et al. 2017) has been reported to parasitise nematode cysts and eggs.

Grant and Elliott (1984) reported *Monocillium* sp. parasitising the cysts of the soybean cyst nematode *Heterodera glycines*. This is so far the only report on *Monocillium* antagonising a plant parasitic nematode. The genus *Monocillium* Saksena, 1955 was emended and placed in the Niessliaceae by Gams (1971), and *Monocillium* spp. were regarded as the asexual morphs of the hypocrealean genus *Niesslia* Auersw., 1869. However, the types of both genera have not yet been connected conclusively by elucidation of the life cycle or by molecular data, hence we hesitate to regard these genera as synonymous and treat them as separate taxonomic entities for the time being. The genus *Monocillium* currently comprises eighteen species (http://www.mycobank.org/quicksearch.aspx) and is defined by showing acremonium-like morphology, but is characterised by unbranched conidiophores with phialides having thickened walls in the lower part. The known species were isolated from soil, plant materials such as dead leaves and wood, but also from other fungi, and building material (such as wall paper). Among all *Monocillium* species described so far (Barron 1961; Gams 1971; Gams and Turhan 1996; Girlanda and Luppi-Mosca 1997; Ramaley 2001) *M. curvisetosum* W. Gams & Turhan is the only species which was originally isolated from aphids as an unusual host for this genus. However its potential parasitic association with its host has not yet been reported.

Egg-parasitic fungi attacking cyst nematodes have repeatedly been isolated from all agricultural soils in various geographic regions (Chen and Chen 2002; Dababat et al. 2015).

Experimental wheat fields of the International Maize and Wheat Improvement Centre (CIMMYT) in Turkey, where a significant reduction in population size of the cereal cyst nematode *Heterodera filipjevi* had been observed between two consecutive years (unpublished data), were sampled to isolate and study fungal candidates that could be causally involved in this drop of the nematode population size.

Here we report a so-far undescribed hypocrealean species which destructively parasitised the eggs of *H. filipjevi*. The antagonistic interaction of this fungus with the nematode eggs was studied based on in vitro tests. We also report the antagonistic potential of *M. bulbillosum* as the most closely related species to the herein described fungus, towards the eggs of *H. filipjevi*.

Materials and methods

Sample collection and materials examined

Cysts of *H. filipjevi* were collected from experimental wheat fields of CIMMYT in the Central Anatolian Plateau of Turkey in 2013. The fields located in Yozgat (39°08'N, 34°10'E; altitude 985 m.a.s.l) and Haymana (39°26'N, 39°29'E, altitude 1260 m.a.s.l) were naturally nematode infested. The samples including soil and roots were collected at random from the rhizosphere of wheat plants at the end of the growing season. Cysts were extracted from the collected samples using the modified flotation decanting method (Coyne et al. 2007). From the extracted suspensions, cysts were manually collected under a dissecting microscope and stored in 1.5 ml microtubes at 4 °C either in dry condition or in sterile tap water until further use. For taxonomic and phylogenetic inferences, additional fungal strains were obtained from the Westerdijk Fungal Biodiversity Institute (formerly CBS-KNAW, Utrecht, Netherlands).

Cultural studies

Fungal isolation from eggs of *Heterodera filipjevi*

The field-collected cysts of *H. filipjevi* were scrutinised by using a dissecting microscope to separate symptomatic cysts showing defined discolourations or bearing discernible hyphae, from healthy-looking (i.e. homogeneously brown) or empty cysts. Symptomatic cysts were selected, surface-sterilised in 5% sodium hypochlorite (NaOCl), and dissected to collect their egg contents. Only the nematode eggs showing symptoms of fungal infection were processed for fungal isolation and culture-dependent species identification. A portion of the fungal infected eggs were additionally used for culture-independent identification. The methods applied here, have been described in greater detail in Ashrafi et al. (2017).

Growth rate studies

Growth rates were determined at various temperatures from 15 to 35 °C at 5 °C intervals in the dark or in ambient conditions by placing agar disks (5 mm diam.), excised from the margin of a young potato dextrose agar (PDA) culture onto five replicate plates of PDA, cornmeal agar (CMA), oatmeal agar (OA; 30 g oatmeal, 18 g agar-agar, 1L deionised water), synthetic nutrient-poor agar (SNA; Nirenberg (1976)), and malt extract agar (MEA). The colony diameter was measured weekly for a 3 week period. Colour changes of fungal structures formed in culture were checked using 3% potassium hydroxide (KOH) watery solution.

Pathogenicity tests against *H. filipjevi*

The antagonistic potential of the below described species and *M. bulbillosum*, respectively, was assessed towards *H. filipjevi* in vitro as previously described (Ashrafi et al. 2017). Briefly, healthy cysts and eggs were surface-sterilised and placed either on or at the margin of the growing mycelium of one-month-old PDA or 2% water agar (WA) cultures of the two fungal species. To document the process of colonisation of eggs of *H. filipjevi* by the new fungal species, a slide culture technique was also performed using PDA 1/3 strength (compare Ashrafi et al. (2017)).

Microscopy

Nematode eggs and fungal structures were examined and photographed by a Zeiss Axioskop 2 plus compound microscope and an Olympus SZX 12 stereo microscope equipped with a Jenoptik ProgRes® digital camera. Images were recorded using CapturePro 2.8 software (Jenoptic, Jena, Germany). Nematode eggs colonised by fungi, and fungal structures were mounted in water or lactic acid and photographed. Cysts were photographed in water in a square cavity dish (40×40×16 mm). To illustrate different stages of fungal development and fungal colonisation of nematode eggs, slide cultures were prepared (Gams et al. 1998) and then photographed. Nomarski Differential Interference Contrast (DIC) optic was used for observation and measurements. All measurements were taken in water, and are given as x1–x2 (x3 ± SD), with x1 = minimum value observed, x2 = maximum value observed, x3 = average, and standard deviation (SD), followed by the number of measurements (n).

Scanning electron microscopy was performed on a Quanta 250 scanning electron microscope (FEI Deutschland GmbH, Frankfurt, Germany). Fungal structures of interest were obtained from a one-month-old OA culture grown at 23 °C in the dark and directly analysed using environmental scanning electron microscopy (ESEM). For the experiment, pressures between 410 and 490 Pa at 4 °C were employed. For cooling the sample chamber was equipped with a Peltier stage. Fungal mycelia with abundant

conidia were placed on non-conductive double-sided adhesive discs on a flat specimen stub and positioned on the Peltier stage for cooling. Images were taken at acceleration voltage of 12.5 kV. Scanning speed was 60 µsec. For imaging of beam sensitive fungal structures, the scanning modus was changed to 3 µsec with 20-fold line integration. Images were adjusted in brightness and contrast using Adobe Photoshop software CS 5.1.

Molecular phylogenetic studies

DNA extraction, PCR amplification and DNA sequencing

Fungal genomic DNA was isolated from mycelia grown on PDA using a modified CTAB method, and from individual nematode eggs infected by fungi using the Qiagen DNeasy Plant Mini Kit (Qiagen, Hilden, Germany) as reported in Ashrafi et al. (2017).

For each specimen, four nuclear loci were amplified: The internal transcribed spacers including the 5.8S rDNA gene (ITS) using the primers ITS1F (Gardes and Bruns 1993) and ITS4 (White et al. 1990); the 5' end of the ribosomal large subunit (LSU) DNA with the primers LROR (Rehner and Samuels 1994) and LR5 (Vilgalys and Hester 1990); partial RNA polymerase II largest subunit 1 (*rpb1*) using the primers cRPB1af and RPB1cr (Castlebury et al. 2004); and partial translation-elongation factor 1-α (TEF) using the primers EF1-983f and EF1-2218r (Castlebury et al. 2004). All PCR reactions were performed as described previously (Ashrafi et al. 2017) with the following thermal programmes: 95 °C (2 min) for initial denaturation followed by 40 cycles of denaturation at 95 °C (30 s), annealing at 52 °C (ITS), 51 °C (LSU), 54 °C (*rpb1*), and 60 °C (TEF) (40 s), extension at 72 °C (1 min for ITS, LSU and *rpb1*, and 1 min and 20 sec for TEF), and a final extension at 72 °C (10 min). Amplicons were purified using the DNA Clean & Concentrator™-5 kit (Zymo Research Corp., Irvine, California, USA) and sequenced by Eurofins Genomics GmbH, (Ebersberg, Germany) with the same primers as used for PCR amplification. Obtained sequences were assembled, edited and trimmed with Sequencher 5.4.1 (Gene Codes Corporation, Ann Arbor, Michigan, USA) and deposited in GenBank under the following accession numbers: MF681481–MF681514. The sequences generated were compared to sequences available in GenBank using a BLASTn search (http://blast.ncbi.nlm.nih.gov/Blast.cgi) (Altschul et al. 1990).

DNA sequence alignment and phylogenetic inference

The newly generated sequences together with closely related sequences selected as revealed by BLASTn searches were used for phylogenetic analyses (Table 1). The sequences were aligned using the online version of Mafft v.7 (Katoh and Standley 2013). All sequences were aligned using the iterative refinement methods: Sequences of the *rpb1* and TEF gene regions were aligned using the algorithms implemented in L–INS–i, while LSU and ITS were aligned applying the Q–INS–i algorithm. Only

Table 1. Isolates and accession numbers used in the phylogenetic analyses.

Species	Isolate number	Host / substrate	Locality	GenBank accession numbers				Reference
				ITS	LSU	*rpb1*	*tef*	
Bionectria byssicola	CBS 914.97–GML2665	*Alchornea* branches- leaf litter	Uganda, Brazil	AF358252	GQ506011	GQ506040	KX184977	(Hirooka et al. 2010; Moreira et al. 2016; Schroers 2001)
Hyaloseta nolinae	CBS109837	*Nolina micrantha*, leaf litter	USA, New Mexico	KM231846	KM231726	KM232279	–	(Lombard et al. 2015)
Ijuhya vitellina	DSM104494	*Heterodera filipjevi*, egg	Turkey	KY607535	KY607549	KY607576	–	(Ashrafi et al. 2017)
Monocillium bulbillosum	CBS344.70	mouldy wallpaper	Germany	MF681488	MF681501	MF681513	MF681507	This study
Monocillium gamsii	DSM105458	*Heterodera filipjevi*, egg	Turkey	MF681485	MF681496	MF681512	MF681506	This study
Monocillium gamsii	DSM105459	*Heterodera filipjevi*, egg	Turkey	MF681483	MF681493	MF681511	MF681505	This study
Monocillium gamsii	DSM105460	*Heterodera filipjevi*, egg	Turkey	MF681482	MF681492	MF681510	MF681504	This study
Monocillium gamsii	DSM105461	*Heterodera filipjevi*, egg	Turkey	MF681481	MF681490	MF681509	MF681503	This study
Monocillium ligusticum	CBS684.95	ectomycorrhizae of *Pinus halapensis*	Italy	MF681489	MF681502	MF681514	MF681508	This study
Nisslia exilis	CBS357.70	*Picea abies*, bark	Germany	–	AY489718	AY489645	AY489613	(Castlebury et al. 2004)
Nisslia exilis	CBS560.74	*Pinus sylvestris*, decayed needle	England	–	AY489720	AY489647	AY489614	(Castlebury et al. 2004)

the start and end of the alignments were trimmed manually in Se-Al v2.0 (Rambaut 1996). The following phylogenetic analyses were applied: a Bayesian method of phylogenetic inference using Metropolis Coupled Monte Carlo Markov chains (MC^3) as implemented in the computer program MrBayes v3.2 (Huelsenbeck and Ronquist 2001; Ronquist and Huelsenbeck 2003). We used MrModeltest v2.2 (Nylander 2004) to determine the best fitting DNA substitution model for the Bayesian approach. Both the hierarchical likelihood ratio test (hLRT) and the Akaike Information Criterion (AIC) selected the general time reversible model of DNA substitution with gamma distributed substitution rates and invariate sites (GTR+I+G) as the best fitting model for all individual data sets and was implemented for the analyses accordingly. For the Bayesian analyses four incrementally heated simultaneous Monte Carlo Markov chains were run with 2.000.000 generations using random starting trees and flat *prior* distributions. Trees were sampled every 500 generations resulting in a total of 4001 sampled trees. A 50% majority rule consensus tree was computed only from trees of the plateau, and if, additionally, the split frequencies were below 0.01. Thus, 501 trees were discarded as "burnin". Maximum likelihood (ML) analyses were performed using RAxML 7.2.8 (Silvestro and Michalak 2012; Stamatakis 2014) implemented in Geneious 8.1.2 applying the general time-reversible (GTR) substitution model with gamma model of rate heterogeneity and 1000 replicates of rapid bootstrapping. Neighbor-joining (NJ) analyses (Saitou and Nei 1987) was

done in PAUP 4.0b10 in the batch file mode (Swofford 2002) applying the Kimura two-parameter model of DNA substitution (Kimura 1980) with a transition/transversion ratio of 2.0 to compute genetic distances. Support for internal nodes was estimated by 1000 bootstrap replicates (Felsenstein 1985). Two members of Bionectriaceae, *Bionectria byssicola* (Berk. & Broome) Schroers & Samuels and *Ijuhya vitellina* Ashrafi, W. Maier & Schroers, were selected as outgroup to root the trees. The phylogenetic trees were visualised using FigTree v. 1.4.2 (http://tree.bio.ed.ac.uk/software/figtree).

Results

Sample collection and fungal isolation

Among the field-collected samples, a high proportion of cysts was found containing blackish bodies resembling microsclerotia-like structures upon microscopy (Fig. 1A). By dissecting the infected cysts, microsclerotia-like black bodies were found to be colonising the individual nematode eggs (Fig. 1B, C). In some infected eggs the developing juveniles were found to be entirely destroyed exhibiting an olivaceous brownish appearance (Fig. 1D, E). Eggs were colonised by one or occasionally two microsclerotia. When cultured on PDA, hyphae grew out of the microsclerotia of the infected eggs (Fig. 1F), and formed colonies at first white creamy, later becoming blackish dotted centrally with a general dark appearance due to the dense pigmentation (Fig. 1G).

Sequence comparison and phylogenetic inference

The DNA sequences of four different gene regions obtained from the examined specimens of the here described nematode-parasitic fungus were either identical (in TEF and RPB1), or nearly identical (1 base pair (bp) substitution in LSU, and up to 2 bp substitutions in ITS). The most similar DNA sequences found in GenBank using BLASTn searches belonged to *Hyaloseta nolinae*, the sexual morph of *Monocillium nolinae*, and shared similarities of 96% in the ITS region, 99% in the LSU, and 89% in *rpb1*. A similar BLASTn search in MycoBank showed identities of the ITS sequence of 96.6% with *M. bulbillosum*, 93.9% with *H. nolinae* and 92.7% with *Niesslia exosporioides*, and of the LSU sequence of 99.5% with *H. nolinae*, and 99% with both *M. bulbillosum* and *Niesslia exosporioides* suggesting a close relationship with the representatives of the Niessliaceae. Fungal DNA could also be directly isolated and sequenced from individual eggs displaying the typical symptoms of fungal infection. These DNA sequences were identical to the sequences retrieved from pure cultures supporting the conspecificity of the symptom-causing structures within the egg with the isolated pure cultures derived from the eggs.

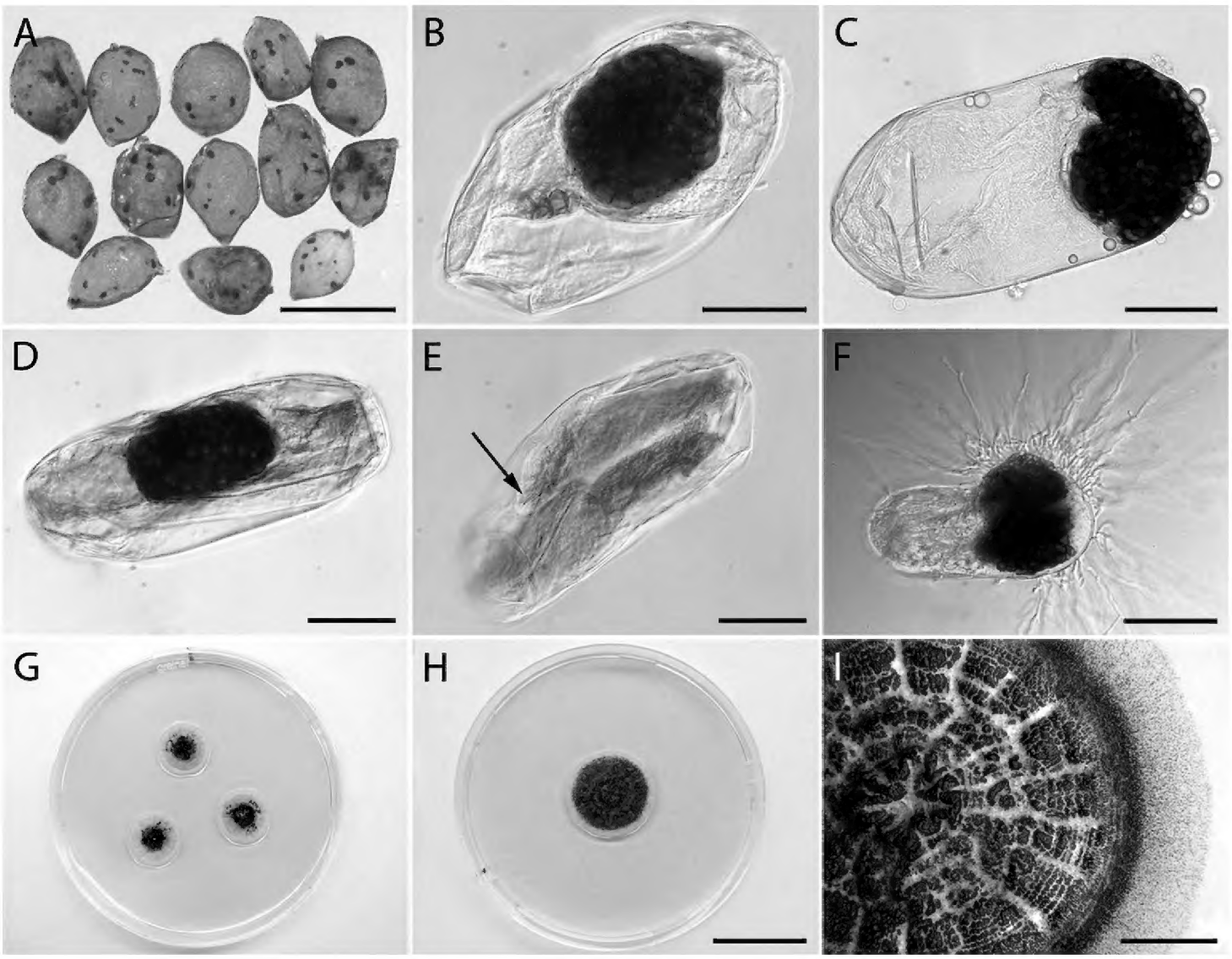

Figure 1. Naturally infested cysts and eggs of *Heterodera filipjevi* with *Monocillium gamsii*, and pure cultures obtained from infected eggs. **A** Field collected symptomatic cysts bearing parasitised eggs. **B–E** Nematode eggs infected by *M. gamsii* **B, D** Nematode eggs containing microsclerotia of *M. gamsii* **E** An embryonated egg containing a second stage juvenile (J2) parasitised by *M. gamsii* (arrow points at nematode's stylet) **F** A nematode egg containing microsclerotia, and hyphae growing out of it **G–H** colony of *M. gamsii* grown on PDA **G** colonies developing from three individually plated infected eggs **H** A 25-d-old culture grown at 25 °C in the dark **I** The surface of a five-month-old culture detailing the sclerotioid masses covering the colony surface. Single microsclerotia can be seen as little black dots at the margin of the culture. Scale bars: 800 µm (**A**); 30 µm (**B–E**); 50 µm (**F**); 2 cm (**H**); 5 mm (**I**).

The final combined ITS, LSU, *rpb1* and *tef* dataset comprised 11 strains representing 7 species with a total alignment length of 2949 bp (603 ITS, 797 LSU, 649 *rpb1*, 900 *tef*). The topologies of the phylogenetic trees were identical using Bayesian inference (Fig. 2), neighbor-joining or maximum likelihood (not shown). The four sequenced strains of the here described nematode egg-colonising fungus were recovered as a highly supported monophyletic group with a close sister group relationship to *M. bulbillosum* and with *H. nolinae* as the next-closest relative. In the second monophyletic clade of Niessliaceae, two strains of the type species of *Niesslia*, *N. exilis*, proved to be paraphyletic with respect to *M. ligusticum* (Fig. 2).

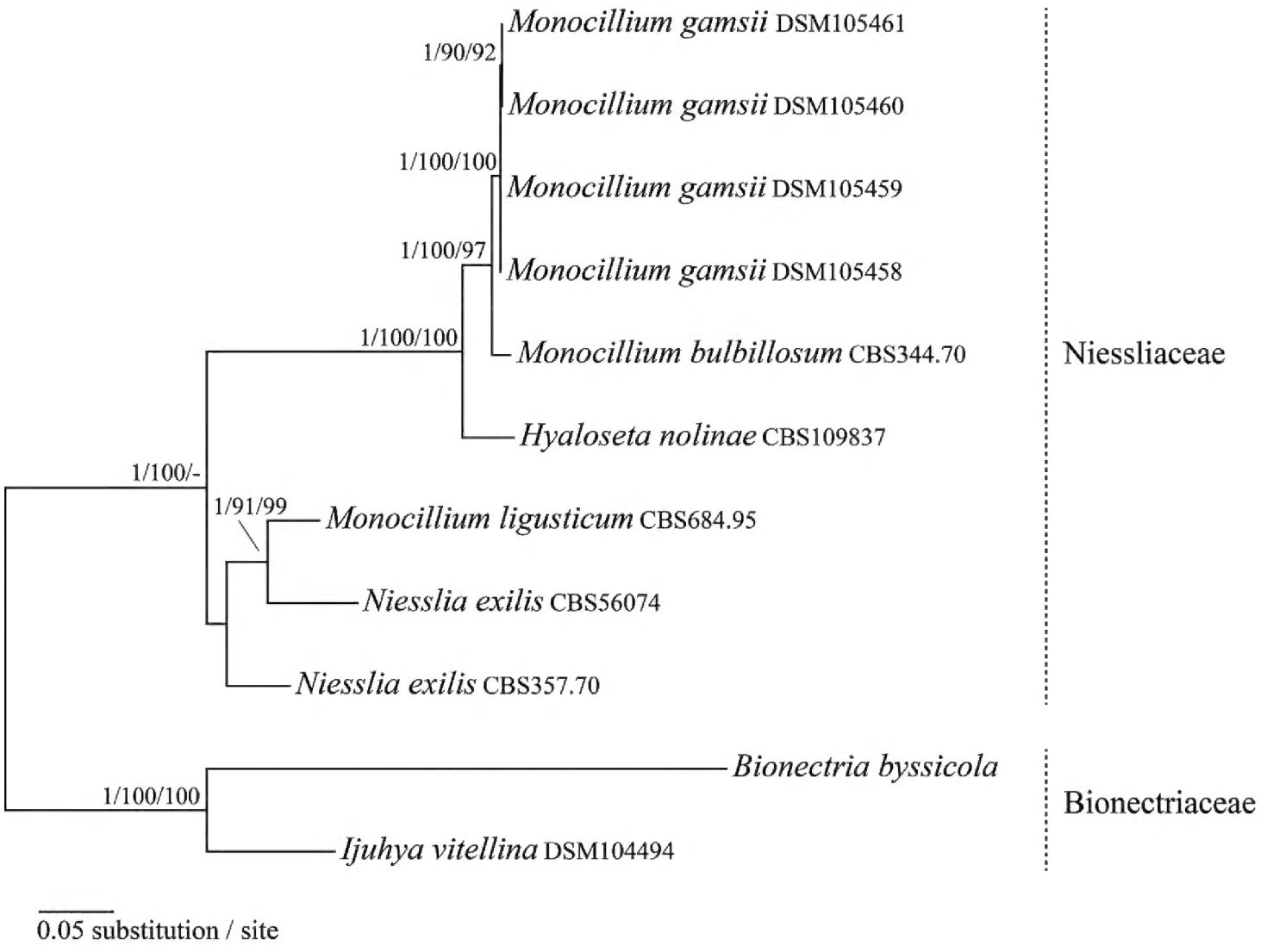

Figure 2. Bayesian inference of phylogenetic relationships using four strains of the here described nematode parasite and all Niessliaceae present in GenBank based on an alignment of ITS, LSU, *rpb1*, and *tef* sequences using GTR+I+G as nucleotide substitution model. Depicted is a 50% majority rule consensus tree derived from 3500 trees from the stationary phase of a Monte Carlo Markov Chain. *A posteriori* probability (BIpp) values greater than 0.95, and bootstrap values of neighbor-joining (NJBT) and maximum likelihood (MLBT) analyses greater than 0.7 are given above branches (BIpp/NJBT/MLBT). Two representatives of the Bionectriaceae, *Bionectria byssicola* and *Ijuhya vitellina*, were used to root the tree.

Taxonomy

***Monocillium gamsii* Ashrafi & W. Maier, sp. nov.**
MycoBank No: MB 823248
Figs 1H, I, 3

Holotype. Turkey, Yozgat, experimental wheat field: dried culture on PDA, originating from an individual egg from a cyst of *Heterodera filipjevi*, isolated by Samad Ashrafi, August 2013, dried culture on PDA, deposited at the herbarium of the Botanic Garden and Botanical Museum Berlin-Dahlem: B700016491.

Ex-holotype strain: DSM 105458, deposited in the open collection of the Leibniz-Institut DSMZ Deutsche Sammlung von Mikroorganismen und Zellkulturen

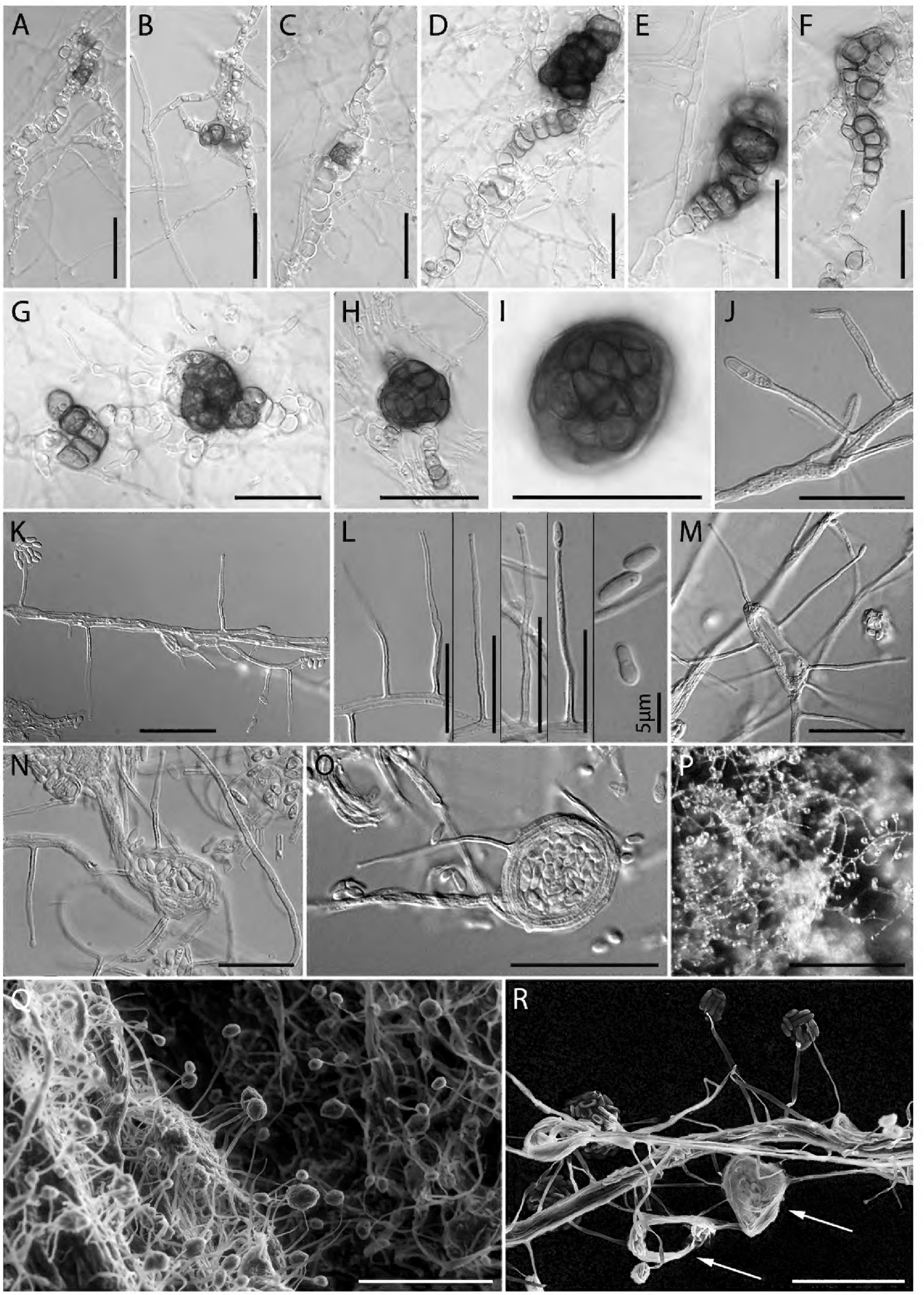

Figure 3. Micrographs of *Monocillium gamsii*. **A–C** Hyphal growth by intercalary development of chlamydospore and dityochlamydospore-like structures filled with guttules **D–H** initiation of microsclerotia by interweaving or coiling of dictyochlamydospores, and growth to full size **I** Highly pigmented sclerotium at maturity displaying a *textura angularis* on surface view **J–N** Setae, phialides and conidia **M–O** Formation of phialides on coiling hyphae **P** Conidial heads, conidia cohering in wet heads **Q, R** SEM: **Q** Phialides from mycelium with conidial heads, arising from hyphae **R** coiling hyphae (arrows), and detail of phialides bearing conidia **A–I** from PDA 1/3 strength **J–P** from PDA; **Q, R** from OA. Scale bars: 30 µm (**A, H, I, K, M, O, R**); 20 µm (**B–G, J, L, N**); 200 µm (**P**), 50 µm (**Q**).

GmbH, GenBank accession numbers: ITS: MF681485; LSU: MF681496; *rpb1*: MF681512; *tef*: MF681506.

Additional material examined. From the same location: DSM 105459 (dried culture on PDA, B700016492), GenBank accession number: MF681483 (ITS), MF681493 (LSU), MF681511 (*rpb1*), MF681505 (*tef*); DSM 105460 (dried culture on PDA, B700016493), GenBank accession number: MF681482 (ITS), MF681492 (LSU), MF681510 (*rpb1*), MF681504 (*tef*); DSM 105461, GenBank accession number: MF681481 (ITS), MF681490 (LSU), MF681509 (*rpb1*), MF681503 (*tef*); and CBS 141176.

Etymology. In honour and memory of Prof Walter Gams for his outstanding works on the genera *Monocillium* and *Niesslia*.

Diagnosis. Naturally occurring infected eggs often accommodating one subglobose, strongly pigmented, dark brownish microsclerotium.

Description. Colonies slow-growing, at 20 °C on PDA reaching 10–12 mm diam. (7d), 19–22 mm (14 d), 25–32 (21 d); optimum temperature for growth 25 °C, 14–16 mm (7 d), 22–25 mm (14 d), 31–34 mm (21d); at 30 °C 10–11 mm (7d), 15–17 (14 d), 22–25 mm (21 d), no growth observed at 35 °C; optimum temperature for growth in other examined cultural media 25 °C, after 21 d reaching 31–32 mm diam. (CMA), 36–40 mm (MEA), 40–50 mm (OA), 32–40 mm (SNA); colonies on PDA finely wrinkled, slightly elevated centrally, first pale creamy, later centrally becoming dotted, greyish-brown to fuscous black due to formation of darkly pigmented microsclerotia, margins and reverse pale creamy. Vegetative hyphae hyaline, thin-walled, forming strands or coils, often with dictyochlamydospore-like structures, occasionally bearing setae with elongate, ellipsoid tips, variable in size. Chlamydospores or dictyochlamydospores mostly developing intercalary, filled with small guttules, gradually pigmented, turning brownish firstly at cell walls, interweaving to form microsclerotia. Cells of microsclerotia angular, pigmented, first pale olivaceous brown filled with guttules, later dark brown, forming a *textura angularis* in surface view. Guttules often absent in mature and strongly melanised sclerotial cells. Microsclerotia later covering the entire colony, developing sclerotioid masses, not changing colour in KOH. Phialides often separated from hyphae by a basal septum, thick-walled in the lower part, the wall thickening distinct at about 1/3 to 1/2 of the total length from the base, thin-walled from ca. midpoint extending to the tip, occasionally slightly inflated in the middle part, gradually tapering to the tip, 21–39 µm (28.7 ± 4.4) in length, 1.0–2.1 µm (1.4 ± 0.2) wide at the base (n = 90), solitary, arising directly from hyphae or hyphal rope, occasionally arising from hyphal coils surrounding several conidia. Conidiogenesis abundant, conidia hydrophilic, adhering in watery droplets, oblong, rarely clavate or ampulliform, one-celled, smooth-walled, 4.1–7.4 × 1.4–2.9 µm (4.9 ± 0.6 × 2.1 ± 0.3) (n = 250). Sexual morph not observed.

Development of *M. gamsii* in nematode eggs in vitro

Monocillium gamsii infected cysts and eggs of *H. filipjevi* in vitro. Initial indications of infection were observed in healthy nematode cysts placed on the fungal colonies

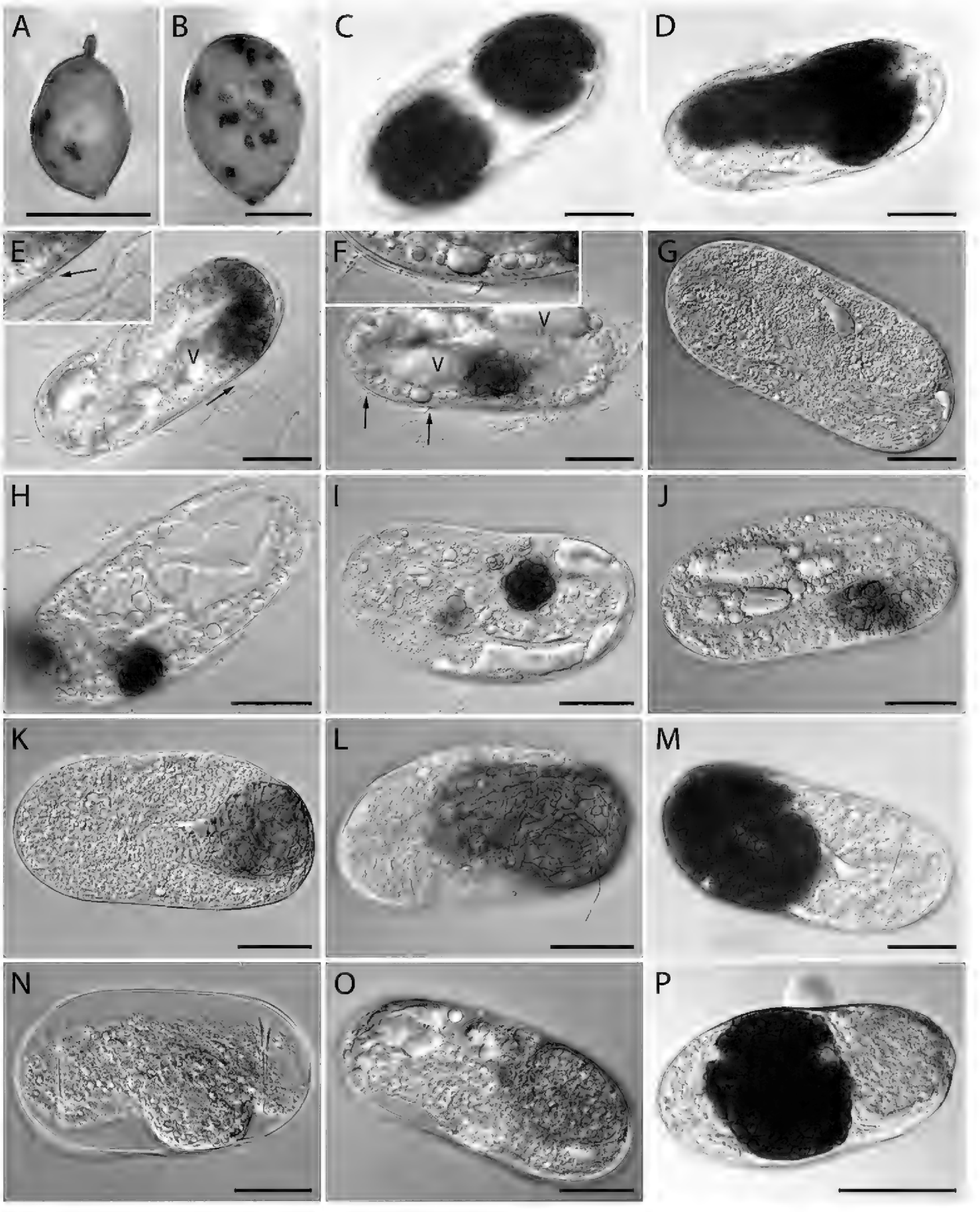

Figure 4. Cysts and eggs of *Heterodera filipjevi* infected by *Monocillium gamsii* exhibiting colonisation in vitro. **A, B** infected cysts rendered black-dotted due to fungal-colonised eggs containing microsclerotia **C, D** Eggs with mature sclerotia, extracted from symptomatic cysts **E, F** Individual hyphae penetrating eggshell (arrows indicate the individual hyphae; V indicates vacuole-like structures) **G–M** Fungal development inside the eggs **G, H** Earlier stages of infection in unembryonated eggs **I, J** Fungal development in the body cavity of developing juveniles where enlarged, thick-walled cells are formed and coalesce to initiate microsclerotia formation **K–M** Microsclerotia developing to full size and pigmentation **N–P** Pigmentation in microsclerotia from pale-olivaceous to darkly brown. Scale bars: 600 μm (**A**); 300 μm (**B**); 30 μm (**C–O**); 50 μm (**P**).

within 2–3 weeks (Fig. 4A, B). The fungus rendered the homogenously brown healthy looking cysts black-dotted, bearing a strong resemblance to the naturally infected cysts collected from fields. By dissecting the symptomatic cysts, nematode eggs were found to be colonised with darkly pigmented spherical to subglobous microsclerotia formed inside the body cavity of the developing juveniles (Fig. 4C). Similar to some naturally infected eggs, sclerotioid masses were also found in some artificially infected samples colonising almost the entire egg (Fig. 4D).

In the slide cultures, fungal infection of eggs was initiated by individual hyphae directly penetrating the eggshell and body cuticle of developing juveniles (Fig. 4E, F). Following penetration, filamentous hyphae entirely colonised the unembryonated eggs (Fig. 4G, H) or the body cavity of the developing juveniles (Fig. 4I, J), enlarged (Fig. 4H–J), occasionally inflated, forming thick-walled, finely pigmented, and guttules-filled cells (Fig. 3J), which eventually coalesced to form discrete microsclerotia with a *textura angularis* appearance (Fig. 4K–M). Infection studies revealed that such microsclerotia could be formed 7–10 d after the incubation of nematode eggs with the fungus.

Pigmentation of microsclerotia occurred during fungal development from hyaline to olivaceous brown and later strongly brownish melanised cells (Fig. 4N–P). Microsclerotia developing inside the artificially infected eggs displayed a *textura angularis* and were indistinguishable from those found in the naturally infected samples. At the early stages of development, microsclerotial cells were often filled with guttules (oil-like bodies), which were not observed in the mature microsclerotia. At the early stages of fungal infection (up to 10 d after inoculation), some vacuole-like structures were observed inside the eggs along the body cavity of developing juveniles (cf. Fig. 4E, F) with a glistening reflexive appearance, which were not observed at later stages of development, or in the field collected samples containing mature sclerotia.

Parasitism of *M. bulbillosum* towards *H. filipjevi*

The antagonistic potential of *M. bulbillosum* was also examined against *H. filipjevi* in vitro. Eggs of *H. filipjevi* were infected by *M. bulbillosum* in the course of 2–4 weeks. The infection symptoms were similar to the symptoms described for *M. gamsii*. *Monocillium bulbillosum* rendered cysts black dotted, containing eggs colonised with microsclerotia. In early stages of infection, eggs were entirely colonised with filamentous hyphae which later developed into microsclerotia with a *textura angularis* on the surface (Fig. 5A–F).

Discussion

The results obtained from comparative morphological characteristics and molecular phylogenetic inference using four gene regions, suggested *M. gamsii* as a new species. Within the genus *Monocillium*, only *M. bulbillosum*, *M. curvisetosum*, *M. indi-*

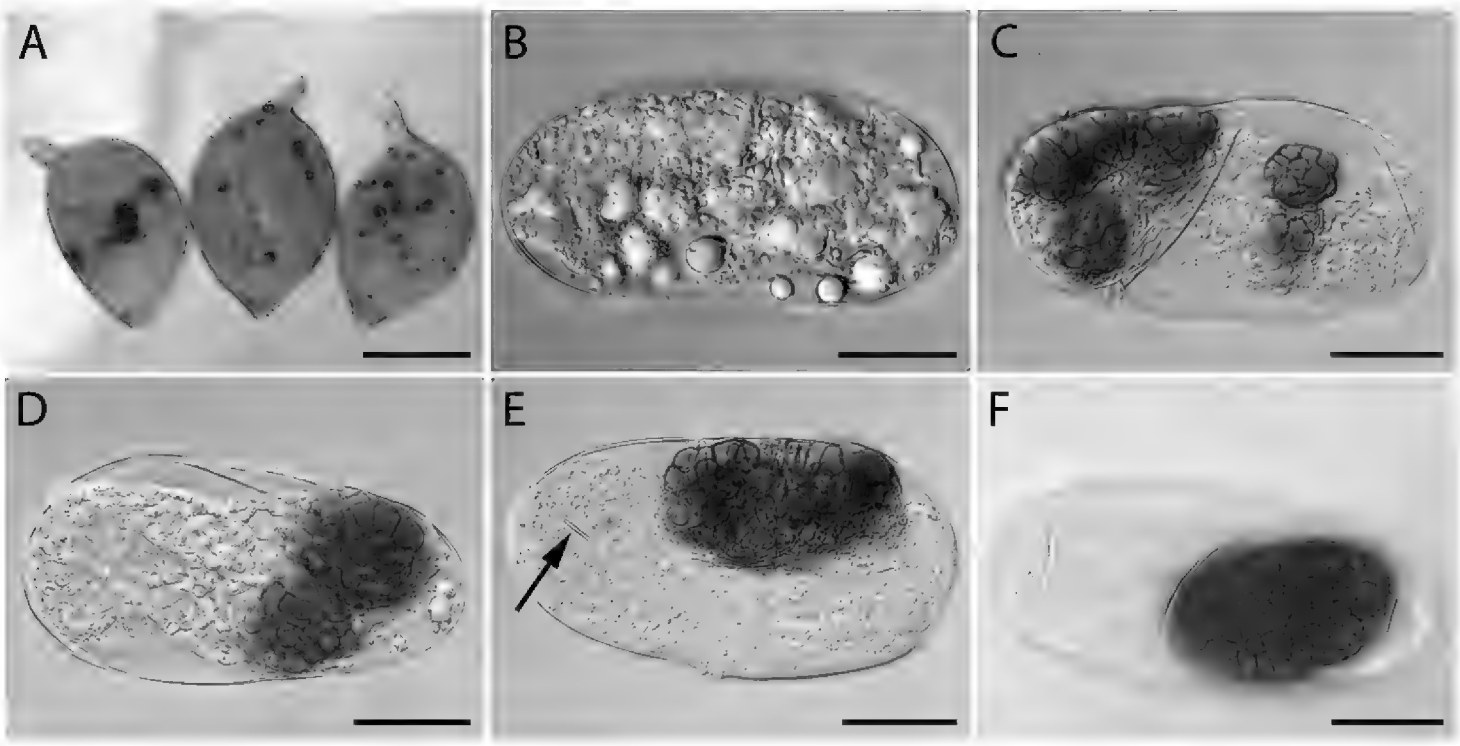

Figure 5. Cysts and eggs of *Heterodera filipjevi* infected by *Monocillium bulbillosum* in vitro. **A** Symptomatic cysts infected by *M. bulbillosum* **B** Infected egg showing early stage of fungal colonisation **C–F** Formation of microsclerotia in nematode eggs (arrow points at nematode's stylet). Scale bars: 300 µm (**A**); 30 µm (**B–F**).

cum and *M. ligusticum* have been reported to form (micro-) sclerotia in culture, as is also the case in *M. gamsii*. In the (micro-) sclerotia forming group, *M. gamsii* can be separated from *M. indicum* by producing conidia cohering in watery heads instead of dry conidia. *Monocillium curvisetosum* produces dry and globose conidia, while *M. gamsii* produces oblong and watery conidia. The new taxon differs from *M. ligusticum* by having much shorter phialides: 21–39 µm vs (35–) 40–70 (–140) µm (Girlanda and Luppi-Mosca 1997). The difference between these two species is also strongly supported by sequence comparison (Fig 2). According to phylogenetic inference, *M. bulbillosum* is very closely related to but separable from *M. gamsii*. Both *M. gamsii* and *M. bulbillosum* form microsclerotia in culture, however *M. bulbillosum* forms mainly bulbillose and individually distinct microsclerotia while these structures in *M. gamsii* are mostly confluent and non-separable. *Monocillium gamsii* grows slightly faster in comparative growth tests on PDA. In addition, *M. gamsii* forms setae, and its conidia are clearly longer than those of *M. bulbillosum* (4.1–7.4 × 1.4–2.9 µm vs 2.9–3.5 × 1.8–2.1 µm). They also differ clearly by the habitat they were originally isolated from. While *M. gamsii* was isolated from the eggs of nematodes in a semiarid region in the Central Anatolian plateau of Turkey, *M. bulbillosum* was isolated only once from wall paper in Kiel Germany (Gams 1971). Interestingly though, *M. bulbillosum* was also able to parasitise eggs of *H. filipjevi* in our in vitro assays and formed microsclerotia in the infected eggs in a similar manner as *M. gamsii*.

Hyaloseta nolinae (asexual morph: *Monocillium nolinae*) was included in this study according to a BLASTn search in GenBank, showing a high sequence similarity with the sequences of *M. gamsii* as query. In the phylogenetic analyses presented here it forms a highly supported monophyletic group with *M. gamsii* and *M. bulbillosum* (Fig. 2). In contrast to *M. gamsii*, *M. nolinae* (the asexual morph of *H. nolinae*) does not form

microsclerotia in culture. *Hyaloseta* Ramaley, 2001 was described as a monotypic genus from Asparagaceae (formerly Agavaceae) in New Mexico developing both conidia and ascomata on the fibrous leaves of its host (Ramaley 2001). According to the limited phylogenetic evidence presented here *M. gamsii* and *M. bulbillosum* could be transferred to the holomorph genus *Hyaloseta*. However, the differential characters used to define *Hyaloseta* in comparison to *Niesslia* are subtle. Therefore, as long as an extensive molecular phylogenetic analysis of all representatives of *Niesslia* and *Monocillium* is pending, it seems less disruptive to place the new species in the 'anamorph genus' *Monocillium*.

It is intriguing that microsclerotia, which represent the main symptoms of fungal infection of nematode cysts and eggs in both *M. bulbillosum* and *M. gamsii* were readily reproduced in fungal pure cultures and were also formed in artificially infected nematode eggs. Apart from the essential role of conidia in fungal reproduction and dispersal, it seems that microsclerotia also play an important part in the developmental cycle of these fungi, at least with respect to those parts of their life cycle that could be assayed in vitro here and during which it interacts with nematodes. *Monocillium gamsii* was found in field-collected dried cysts in the semiarid Central Anatolian Plateau. In nature, fungal sclerotia are generally considered as resting structures by which the fungus may tolerate abiotic stresses like dessication, and can thus survive until favourable conditions return. Support for this hypothesis comes from the observation that we were able to isolate *M. gamsii* from field-collected cysts obtained by culturing the microslerotium-containing infected eggs that had been kept for more than one year in dry conditions either at 4 °C or at room temperature. Furthermore, nematode cysts are protective structures in which nematode eggs can survive for many years in soil in the absence of host plants or in adverse environments. By colonising the cyst contents, i.e. the mucilaginous matrix and the eggs, the egg-colonising fungi for example *M. gamsii* and *M. bulbillosum*, may thus benefit from this "specific" niche where they may have equivalent prolonged-survival conditions.

Our microscopic observations of the in vitro tests revealed that *M. gamsii* is capable of destructively and quickly parasiting the nematode eggs within the cysts first by penetrating the eggshell, followed by profilic formation of microsclerotia. We did not observe formation of any specific infecting structure like in the case of the recently described cyst and egg-parasitic fungus *Ijuhya vitellina* which developed appressoria (Ashrafi et al. 2017). Incubation of cysts on the colony of *M. bulbillosum* demonstrated that this species can also parasitise the nematode eggs in a similar manner, and even form microsclerotia. These observations suggest that both species may be candidates for nematode biocontrol.

Acknowledgements

This work was finacially supported by the Federal Ministery for Economic Cooporation and Development, Germany, Grant ID: W0267 GIZ/BMZ-Endophyte as Biocontrol. Additional support of the International Maize and Wheat Improvement Centre (CIMMYT) and the Julius Kühn-Institut are gratefully acknowledged. Special thanks go to

the Fiat Panis Foundation, Ulm, Germany, for a "PhD completion stipend" to SA. We thank Dr Thomas Kühne for carefully reading the manuscript, and Anke Brisske-Rode and Katrin Balke for technical support in the molecular studies and culture maintaining.

References

Altschul SF, Gish W, Miller W, Myers EW, Lipman DJ (1990) Basic Local Alignment Search Tool. Journal of Molecular Biology 215: 403-410. https://doi.org/10.1006/jmbi.1990.9999

Ashrafi S, Helaly S, Schroers HJ, Stadler M, Richert-Poeggeler KR, Dababat AA, Maier W (2017) *Ijuhya vitellina* sp. nov., a novel source for chaetoglobosin A, is a destructive parasite of the cereal cyst nematode *Heterodera filipjevi*. PloS ONE 12: e0180032. https://doi.org/10.1371/journal.pone.0180032

Baral H-O, Weber E, Gams W, Hagedorn G, Liu B, Liu X, Marson G, Marvanová L, Stadler M, Weiß M (2017) Recommendations about generic names to be protected or suppressed in the Orbiliaceae (Orbiliomycetes). Mycological Progress. https://doi.org/10.1007/s11557-017-1300-6

Barron GL (1961) *Monocillium humicola* sp. nov. and *Paecilomyces variabilis* sp. nov. from soil. Canadian Journal of Botany 39: 1573–1578. https://doi.org/10.1139/b61-137

Castlebury LA, Rossman AY, Sung GH, Hyten AS, Spatafora JW (2004) Multigene phylogeny reveals new lineage for *Stachybotrys chartarum*, the indoor air fungus. Mycological Research 108: 864–872. http://dx.doi.org/10.1017/S0953756204000607

Chen F, Chen S (2002) Mycofloras in cysts, females, and eggs of the soybean cyst nematode in Minnesota. Applied Soil Ecology 19: 35–50. http://dx.doi.org/10.1016/S0929-1393(01)00179-2

Coyne DL, Nicol JM, Claudius-Cole B (2007) Practical plant nematology: a field and laboratory guide. SP-IPM Secretariat, International Institute of Tropical Agriculture (IITA), Cotonou, Benin, 82 pp.

Dababat AA, Imren M, Erginbas-Orakci G, Ashrafi S, Yavuzaslanoglu E, Toktay H, Pariyar SR, Elekcioglu HI, Morgounov A, Mekete T (2015) The importance and management strategies of cereal cyst nematodes, *Heterodera* spp., in Turkey. Euphytica 202: 173–188. https://doi.org/10.1007/s10681-014-1269-z

Felsenstein J (1985) Confidence limits on phylogenies: an approach using the Bootstrap. Evolution 39: 783–791. https://doi.org/10.2307/2408678

Gams W (1971) Cephalosporium-artige Schimmelpilze (Hyphomycetes). Gustav Fischer Verlag, Stuttgart, Germany.

Gams W, Hoekstra ES, Aptroot A (1998) CBS course of mycology. Baarn Centraalbureau voor Schimmelcultures.

Gams W, Turhan G (1996) An extreme modification of *Monocillium*: *Monocillium curvisetosum* n. sp. Mycotaxon 59: 343–348.

Gardes M, Bruns TD (1993) ITS primers with enhanced specificity for basidiomycetes--application to the identification of mycorrhizae and rusts. Molecular Ecology 2: 113–118. https://doi.org/10.1111/j.1365-294X.1993.tb00005.x

Girlanda M, Luppi-Mosca AM (1997) *Monocillium ligusticum*, a new species from mycorrhizal roots in Mediterranean north Italy. Mycotaxon 67: 265–274.

Grant CE, Elliott AP (1984) Parasitism of *Heterodera glycines* and *Globodera solanacearum* by fungi. First International Congress of Nematology, Canada, 5-10 August. [abstract]

Hirooka Y, Kobayashi T, Ono T, Rossman AY, Chaverri P (2010) *Verrucostoma*, a new genus in the Bionectriaceae from the Bonin Islands, Japan. Mycologia 102: 418–429. https://doi.org/10.3852/09-137

Huelsenbeck JP, Ronquist F (2001) MRBAYES: Bayesian inference of phylogenetic trees. Bioinformatics 17: 754–755. https://doi.org/10.1093/bioinformatics/17.8.754

Katoh K, Standley DM (2013) MAFFT Multiple Sequence Alignment Software Version 7: Improvements in Performance and Usability. Molecular Biology and Evolution 30: 772–780. https://doi.org/10.1093/molbev/mst010

Kerry B (1988) Fungal parasites of cyst nematodes. Agriculture Ecosystems & Environment 24: 293–305. https://doi.org/10.1016/0167-8809(88)90073-4

Kerry BR, Hirsch PR (2011) Ecology of *Pochonia chlamydosporia* in the rhizosphere at the population, whole organism and molecular scales. In: Davies K, Spiegel Y (Eds) Biological control of plant-parasitic nematodes: Building coherence between microbial ecology and molecular mechanisms. Springer Netherlands, Dordrecht, 171–182. https://doi.org/10.1007/978-1-4020-9648-8_7

Khan A, Williams KL, Nevalainen HKM (2006) Infection of plant-parasitic nematodes by *Paecilomyces lilacinus* and *Monacrosporium lysipagum*. BioControl 51: 659–678. https://doi.org/10.1007/s10526-005-4242-x

Kimura M (1980) A simple method for estimating evolutionary rates of base substitutions through comparative studies of nucleotide sequences. Journal of Molecular Evolution 16: 111–120. https://doi.org/10.1007/BF01731581

Kühn J (1877) Vorläufiger Bericht über die bisherigen Ergebnisse der seit dem Jahre 1875 im Auftrage des Vereins für Rübenzucker-Industrie ausgeführten Versuche zur Ermittlung der Ursache der Rübenmüdigkeit des Bodens und zur Erforschung der Natur der Nematoden. Zeitschrift des Vereins für die Rübenzucker-Industrie des Duetschen Reich (ohne Band) 27: 452–457.

Lombard L, van der Merwe NA, Groenewald JZ, Crous PW (2015) Generic concepts in Nectriaceae. Stud Mycol 80: 189–245. https://doi.org/10.1016/j.simyco.2014.12.002

Lopez-Llorca LV, Maciá-Vicente JG, Jansson H-B (2008) Mode of action and interactions of nematophagous fungi. In: Ciancio A, Mukerji KG (Eds) Integrated management and biocontrol of vegetable and grain crops nematodes. Springer Netherlands, Dordrecht, 51–76. https://doi.org/10.1007/978-1-4020-6063-2_3

Moreira GM, Abreu LM, Carvalho VG, Schroers H-J, Pfenning LH (2016) Multilocus phylogeny of *Clonostachys* subgenus *Bionectria* from Brazil and description of *Clonostachys chloroleuca* sp. nov. Mycological Progress 15: 1031–1039. https://doi.org/10.1007/s11557-016-1224-6

Nirenberg H (1976) Untersuchungen über die morphologische und biologische Differenzierung in der *Fusarium*-Section *Liseola*. Mitteilungen der Biologischen Bundesanstalt für Land- und Forstwirtschaft 169: 1–117.

Nordbring-Hertz B, Jansson H-B, Tunlid A (2011) Nematophagous fungi. Encyclopedia of life sciences. John Wiley & Sons, Ltd. https://doi.org/10.1002/9780470015902.a0000374.pub3

Nylander J (2004) MrModeltest v2. Program distributed by the author. Evolutionary Biology Centre, Uppsala University.

Ramaley AW (2001) *Hyaloseta nolinae*, its anamorph *Monocillium nolinae*, and *Niesslia agavacearum*, new members of the Niessliaceae, Hypocreales, from leaves of Agavaceae. Mycotaxon 79: 267–274.

Rambaut A (1996) Se-Al: Sequence Alignment Editor, 2.0a11. http://evolve.zoo.ox.ac.uk and http://tree.bio.ed.ac.uk/software/seal/

Rehner SA, Samuels GJ (1994) Taxonomy and phylogeny of *Gliocladium* analyzed from nuclear large subunit ribosomal DNA-sequences. Mycological Research 98: 625–634. https://doi.org/10.1016/S0953-7562(09)80409-7

Rodríguez-Kábana R, Morgan-Jones G (1988) Potential for nematode control by mycofloras endemic in the Tropics. Journal of Nematology 20: 191–203.

Ronquist F, Huelsenbeck JP (2003) MrBayes 3: Bayesian phylogenetic inference under mixed models. Bioinformatics 19: 1572–1574. https://doi.org/10.1093/bioinformatics/btg180

Saitou N, Nei M (1987) The neighbor-joining method: a new method for reconstructing phylogenetic trees. Molecular Biology and Evolution 4: 406–425.

Schroers HJ (2001) A monograph of *Bionectria* (Ascomycota, Hypocreales, Bionectriaceae) and its *Clonostachys* anamorphs. Stud Mycol: 1–214.

Siddiqui ZA, Mahmood I (1996) Biological control of plant parasitic nematodes by fungi: A review. Bioresource Technology 58: 229–239. https://doi.org/10.1016/S0960-8524(96)00122-8

Silvestro D, Michalak I (2012) raxmlGUI: a graphical front-end for RAxML. Organisms Diversity & Evolution 12: 335–337. https://doi.org/10.1007/s13127-011-0056-0

Stamatakis A (2014) RAxML version 8: a tool for phylogenetic analysis and post-analysis of large phylogenies. Bioinformatics 30: 1312-1313. https://doi.org/10.1093/bioinformatics/btu033

Stirling GR (2014) Biological control of plant-parasitic nematodes: soil ecosystem management in sustainable agriculture. CABI, Wallingford, UK, 510 pp. https://doi.org/10.1079/9781780644158.0000

Swofford DL (2002) PAUP*. Phylogenetic Analysis Using Parsimony (*and Other Methods). Version 4. Sinauer Associates, Sunderland, Massachusetts:

Szabó M, Csepregi K, Gálber M, Virányi F, Fekete C (2012) Control plant-parasitic nematodes with *Trichoderma* species and nematode-trapping fungi: The role of chi18-5 and chi18-12 genes in nematode egg-parasitism. Biological Control 63: 121–128. https://doi.org/10.1016/j.biocontrol.2012.06.013

Tribe HT (1977) Pathology of cyst-nematodes. Biological Reviews of the Cambridge Philosophical Society 52: 477–507. https://doi.org/10.1111/j.1469-185X.1977.tb00857.x

Vilgalys R, Hester M (1990) Rapid genetic identification and mapping of enzymatically amplified ribosomal DNA from several *Cryptococcus* species. Journal of Bacteriology 172: 4238–4246. https://doi.org/10.1128/jb.172.8.4238-4246.1990

White TJ, Bruns T, Lee S, Taylor J (1990) Amplification and direct sequencing of fungal ribosomal RNA genes for phylogenetics. In: Innis M, Gelfand D, Sninsky J, White T (Eds) PCR Protocols: a guide to methods and applications. Academic Press, San Diego, 315–322. https://doi.org/10.1016/B978-0-12-372180-8.50042-1

Zhang S, Gan Y, Xu B, Xue Y (2014) The parasitic and lethal effects of *Trichoderma longibrachiatum* against *Heterodera avenae*. Biological Control 72: 1–8. https://doi.org/10.1016/j.biocontrol.2014.01.009